Brain Tumor Segmentation using Osprey Optimization Assisted DeepLabV3+ Model

Riya Jacob and J. Jenkin Winston*

Department of Electronics and Communication Engineering, Karunya Institute of Technology and Sciences, Coimbatore, Tamil Nadu 641114, India

Abstract: Brain tumors are among the frequently diagnosed malignant conditions across all age groups. Accurately determining their grade has a major challenge for radiologists in clinical assessments and automatic diagnostic systems. Identifying tumor types and implementing preventive measures remains one of the most complex processes of brain tumor classification. Various Deep Learning (DL) models are proposed in the existing approaches for enhancing the accuracy of brain tumor classification. But, the challenges like training time and complexity are occurred in these works. To tackle these issues, this work presents a Enhanced DeepLabV3+ to segment and categorize brain tumor. At first, non-local means (NLM) filtering is utilized for pre-processing for reducing noise and preserving essential structural details. Then, the Enhanced DeepLabV3+ is employed for segmentation, with AlexNet is the backbone for segmentation tasks. To further refine the segmentation process, hyperparameter optimization of the DeepLabV3 architecture is conducted using the Osprey Optimization Algorithm (OOA) approach and provide significant improvements in brain tumor segmentation performance. The evaluation is performed on the Brain TCIA and Figshare datasets and achieved better accuracies of 98.97% and 99.23% respectively.

Keywords: Brain Tumors, Segmentation, AlexNet, Enhanced DeepLabV3+, Hyperparameter Optimization, Osprey Optimization Algorithm.

1. INTRODUCTION

Brain tumors are among the most serious health conditions that affectss individuals worldwide. With respect to the World Health Organization (WHO), brain diseases are classified into different categories, including gliomas and glioblastomas, which are further divided into low grade tumor (LGT) and high-grade tumor (HGT) [1]. LGT, generally called as benign tumors, are less aggressive and do not significantly affect surrounding normal tissues. Then, HGT, also known as malignant tumors, are more severe. They spread rapidly to adjacent brain tissues and have a serious threat to life [2].

For detecting and diagnosing brain tumors at the beginning phase, Magnetic Resonance Imaging (MRI) plays a major part and these modalities help in identifying tumor cells in the brain. This allows for timely medical intervention and improved treatment outcomes. Different MRI image processing techniques are utilized for analyzing the human brain features. This provides high-resolution imaging, enhanced soft tissue differentiation, and improved brightness [3]. Segmenting MRI brain images are important for enhancing diagnostic accuracy. But, the presence of noises, often introduced by image acquisition devices, can complicate the segmentation process [4].

MRI is a highly effective technique for capturing

Different CAD techniques are used for segmenting medical images, with Deep Learning (DL) and classification being prominent examples [8]. DL is exploited for extracting features from images and classification approaches are presented for determining whether a tumor is present. Convolutional Neural Networks (CNNs) outperform traditional methods in accuracy, and the major benefit of CNNs depends in their ability to find important patterns and features from training images [9]. Similarly, architectures like AlexNet, InceptionNet, and EfficientNet have proven

ISSN: 1929-2260 / E-ISSN: 1929-2279/25 © 2025 Neoplasia Research

detailed brain structures; however, the factors like low spatial resolution, inhomogeneity, shape instability, and poor contrast can make the process more complex. Despite these limitations, segmentation remains a reliable and essential pre-processing step in Computer Aided Diagnosis (CAD). Because of the complicated anatomical structure of the brain, MRI images are mainly exploited in different medical applications [5]. Manual segmentation process is costly and timeintensive; due to this, automated segmentation of tumor is preferable, particularly when dealing with large datasets. Despite its advantages, automatic tumor segmentation remains complex because of the significant changes in tumor location, shape, and structure [6]. Hence, implementing automatic tumor segmentation and grading from MRI can provide a valuable, non-invasive alternative for clinical field. This improves the betterment and accuracy in diagnosis of the tumor [7].

^{*}Address correspondence to this author at the Department of Electronics and Communication Engineering, Karunya Institute of Technology and Sciences, Coimbatore, Tamil Nadu 641114, India; E-mail: jenkinwinston@karunya.edu

effective for classification process and has significant potential for detecting brain diseases in clinical images [10]. These models are through a convolution multilayered network, which features several hidden layers and trainable parameters. All MRI input images are passes through a series of convolutional, pooling, filters, and output layers [11].

This work proposes an enhanced DeepLabV3+ model integrated with the Osprey Optimization Algorithm (OOA) for brain tumor segmentation. The model considered non-local means (NLM) filtering for noise removal and AlexNet as the backbone for effective feature extraction. OOA is presented for optimizing hyperparameters of DeepLabV3+, and improves segmentation accuracy and boundary precision. The robustness of the suggested model is validated on two datasets; this demonstrates its potential as a reliable tool for supporting radiologists and advanced automated brain tumor diagnostic systems. The objectives are:

- To present automated brain tumor segmentation and classification using an enhanced models.
- To segment the lesions using DeepLabV3+ and AlexNet is considered as the backbone for segmentation tasks.
- To present metaheuristic OOA approach and provide significant improvements in brain tumor segmentation performance.

The rest sections are: Section 2 presents the recent works based on segmentation of the brain tumor; Section 3 presents the suggested segmentation of the brain tumor; Section 4 presents the analysis of the outcomes and Section 5 ends the work.

2. RELATED WORKS

Recent works based on segmentation of the brain tumor using different approaches like CNN based methods, hybrid approaches, and optimization based methods are listed here:

2.1. CNN based Methods

Ramtekkar et al. [16] presented CNN with different optimizations for brain tumor classification. Here, mean, median and Gaussian filters were used for preprocessing; for achieving segmentation, threshold and histogram were utilized. Then, the Grey level cooccurrence matrix (GLCM) was applied for extracting relevant features. Different metaheuristic optimizations

were used for selecting features and the CNN was used for disease classification.

Farnoosh et al. [15] employed an iterative combination of Spectral Co-Clustering (SCC) and Fuzzy C Means (FCM) for achieving better brain tumor segmentation. For all iterations, SCC identified the tumor blocks and the selected blocks from the prior iteration was used as input for the next step. For the last iteration, FCM was applied to the final chosen block for precisely extracting the tumor and this iterative pseudo-DL process forms a layered structure.

2.2. Hybrid Approaches

Cheng et al. [12] presented Coarse to Fine Feature Model (CFFM) for semantic feature extraction and hierarchical features. Then, the Modality Cross Attentive Model (MCAM) was introduced that extracted complex features from various modalities and maps them into a fused semantic space. This enables the model to learn enriched cross-modal representations. Moreover, the Multi-Scale Context Perception (MSCP) was used for enhancing the ability of the model for capturing important lesions and preserving deep semantic details. Finally, the fusion of fine and coarse grained features provided better feature learning.

Mi et al. [13] presented Diffusion network (DN) with Spatial Channel Attention Infusion (SCAI) and Frequency Spatial Attention (FSA) for achieving segmentation process. The DN was used for extracting multi-scale feature and the SCAI was used for extracting features from encoded layer. Then, the FSA was used for matching the condition features with the DA. At last, the cross model loss was used for supervising the features.

Cekic et al. [14] presented MRI and surgical microscope images for brain tumor classification. The networks like ResNet50 and 101 were utilized in the Mask RCNN model for disease detection. DL models trained from images and the classification outcomes achieved for every patient was integrated with the weighted mean value.

2.3. Optimization based Methods

Devi et al. [17] suggested CNN with Long Short-Term Memory (LSTM) for identifying tumor regions. Here, the Wavelet Packet Transform (SWPT) was applied for extracting relevant features. The Hybrid Adaptive Black Widow based Moth Flame Optimizer (HABW-MFO) was presented for selecting features.

Then, the Adaptive Kernel FCM (AK-FCM) for achieving better brain tumor segmentation.

Mehnatkesh *et al.* [18] demonstrated brain tumor classification using residual learning model. ResNet was combined with an evolutionary algorithm for optimizing the hyperparameters. This existing approach eliminated the need for manual process and the Improved Ant Colony Optimizer (IACO) was used for enhancing optimization performance. This advanced process further improved the model's potential for classifying brain tumors accurately.

Despite these advances, some challenges are present in existing brain tumor segmentation methods. The existing models often achieve high accuracy but at the cost of significant computational demands, restrict their deployment in real-time clinical settings. Some models improve feature extraction and segmentation precision, but have high complexity and longer training times and less scalability. Standard optimizationassisted approaches enhance parameter tuning and performance but still fail with robustness to noise and precise boundary delineation. Thus, current literatures show gaps in robustness, consistent accuracy over diverse datasets and emphasize the need for improved methods. To address these limitations, this work combines the DeepLabV3+ with OOA and aims to achieve improved segmentation accuracy, enhanced robustness and reduced computational cost.

3. PROPOSED MODEL

In medical diagnostics, the segmenting and brain tumors classification is a major part and makes early detection and proper treatment. In this work, the MRI images are pre-processed by the NLM for noise removal and standardizing intensity variations. The DeepLabV3+ model is integrated with the OOA for increasing segmentation performance. The OOA fine-tunes the hyperparameters of DeepLabV3+ and provides optimal feature extraction and segmentation accuracy. Then, the optimized DeepLabV3+ model

segments tumor regions and categorizes lesions into various classes. Figure 1 delineates the architecture of the brain tumor diagnosis process.

3.1. Pre-Processing

The input brain images are resized to 256 × 256 pixels for ensuring consistency in processing. Then, the brain image undergoes a pre-processing step where the Regions of Interest (ROI) are determined for further process. This pre-processing is performed using a NLM filtering, which enhances image quality by minimizing noise and preserving important structural details. Consider a brain dataset \mathcal{D} , has \mathcal{L} brain images and it is given as:

$$D = \left\{ \operatorname{Im}_{n} \quad 1 \le n \le L \right\} \tag{1}$$

where Im_n is the n^{th} image from the D.

3.2. Segmentation

DeepLabV3+ incorporates AlexNet as backbone for enhancing segmentation accuracy by utilizing their corresponding strengths in extracting features and preserving spatial information. As shown in Figure 2, there are two main components DeepLabV3+: encoder and decoder. The encoder is used for extracting features and minimizing feature map dimensionality. Then, the decoder refines edges and restores achieving better segmentation. resolution for DeepLabV3+ effectively separates images integrating Dilated Convolution (DC) and Atrous Spatial Pyramid Pooling (ASPP), which improve boundary recognition. In this network, the AlexNet is backbone network which extracts essential features from the input image. Although, the networks like ResNet and EfficientNet provide higher representation ability, they need substantially high memory and training time. But, AlexNet offered a better balance between accuracy and computational efficiency. Further, AlexNet captures essential feature representations and preserving spatial features necessary for segmentation. By adjusting the

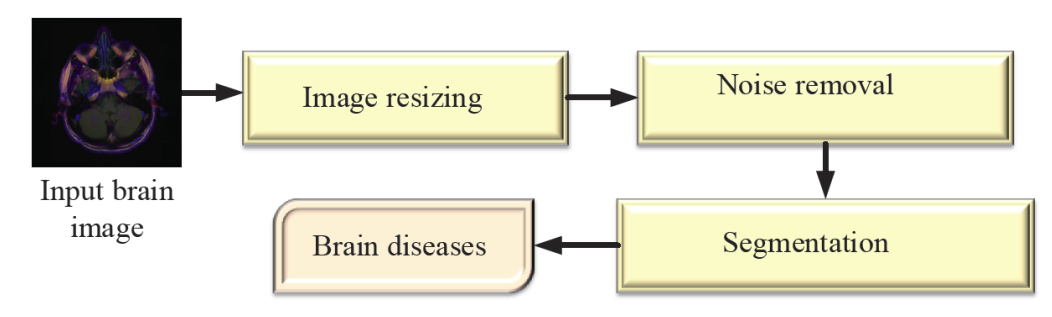


Figure 1: Architecture of the suggested brain tumor diagnosis process.

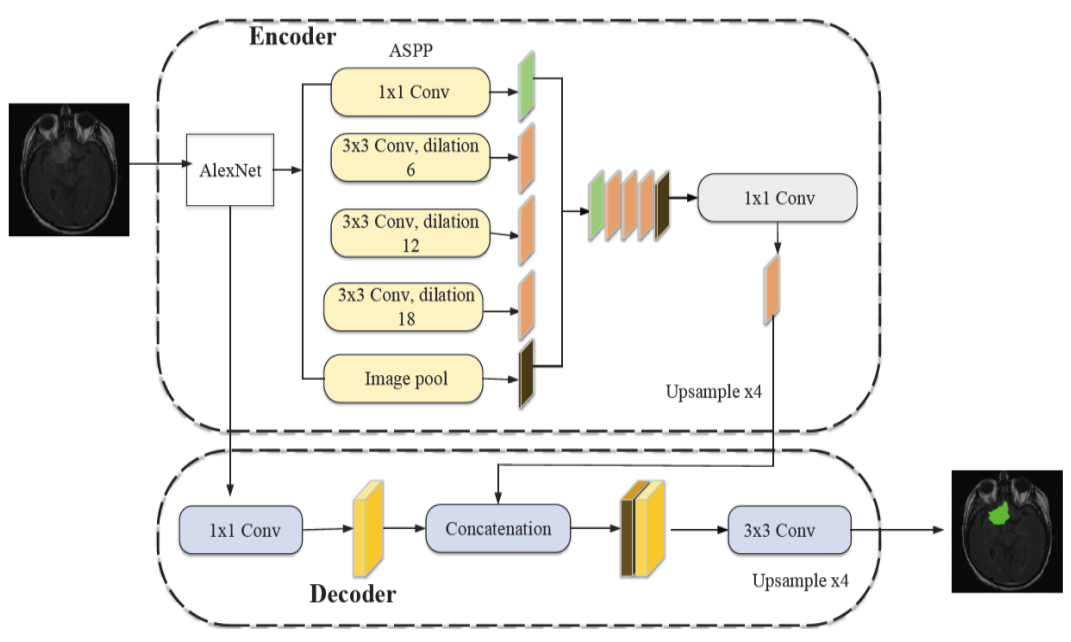


Figure 2: Architecture of DeepLabV3+.

backbone structure, the model enhances spatial and information extraction provides better segmentation performance. DC in the later layers of the backbone network helps in regulating the output feature map's size. The ASPP then categorizes the output image pixels. Finally, the decoder applies convolution for reconstructing transpose segmented image and restoring it to its original dimensions with improved accuracy.

3.2.1. Parameter Optimization

To improve the hyper-parameters the DeepLabV3+, the metaheuristic OOA [19] is presented. The hyper-parameters like backbone network, learning rate, weight decay, dropout rate, loss function and epochs are optimized by the OOA using the fitness function. It is expressed as:

$$fitness = Maximize \left(Dice\ score\right) \tag{2}$$

The OOA mimics the hunting behaviour of ospreys and their strategy to capture fish from the sea. In this, an osprey initially determines the location of its prey before quickly fall to catch it and moving it to a better place. The mathematical modelling of the OOA models this natural hunting behaviour by splitting the optimization process into two key stages: exploration and exploitation. These stages simulate how ospreys search for prey and refine their hunting process. This allows the optimizer to efficiently navigate and optimize complex search spaces. The mathematical modelling of the OOA is explained in this section:

Initialization: Every osprey presents a potential solution by assigning values to the problem parameters with respect to its position within the search space.

$$Y = \begin{bmatrix} Y_1 \\ Y_2 \\ \cdots \\ Y_j \\ \cdots \\ Y_L \end{bmatrix}_{L \times n} = \begin{bmatrix} y_{1,1} & y_{1,j} & \cdots & y_{1,n} \\ z_{2,1} & z_{2,j} & \cdots & y_{2,n} \\ \cdots & \cdots & \cdots & \cdots \\ z_{j,1} & z_{j,k} & \cdots & y_{j,n} \\ z_{2,1} & y_{L,j} & \cdots & y_{M,n} \end{bmatrix}_{L \times n}$$
(3)

where j = 1, 2, 3, ..., L k = 1, 2, 3, ..., n. Here, Y is the Osprey population, Y_i is the j^{th} Osprey, $z_{i,k}$ is the k^{th} dimension, L is the total Osprey and n is the number of dimensions.

Exploration: The hunting stage of the fish is the exploration and Ospreys are powerful predators with better vision. This enables them to detect fish beneath the water's surface. Once they locate their target, they swiftly dive and submerge to capture their prey. This movement improves the exploration capability, helping it locate optimum regions and avoid local optima. In this algorithm, osprey considers other individuals in the population with superior objective function values as fish submerged underwater. The group of fish position FP_i for j^{th} Osprey is determined by:

$$FP_{j} = \left\{ Y_{l} \mid l \in \{1, 2, 3, ..., M\} \land G_{l} < G_{j} \right\} \cup \left\{ Y_{b} \right\}$$
 (4)

where Y_b is the best Osprey.

The osprey selects a target fish at random from the identified set and attack the prey. By simulating the motion of the Osprey to its prey and the new position within the search space is computed as:

$$z_{j,k}^{P1} = z_{j,k} + rand_{j,k} \left(CF_{j,k} - I_{j,k} \times z_{j,k} \right)$$
 (5)

$$z_{j,k}^{P1} = \begin{cases} z_{j,k}^{P1}, low_k \le z_{j,k}^{P1} \le up_k \\ low_k, z_{j,k}^{P1} \le low_k \\ up_k, z_{j,k}^{P1} > up_k \end{cases}$$
 (6)

When the updated position provides a better value, it replaces the osprey's prior position and it is expressed as:

$$Z_{j} = \begin{cases} Z_{j}^{P1}, G_{j}^{P1} < G_{j} \\ Z_{j}, elsewhere \end{cases}$$
 (7)

where Z_j^{P1} is the j^{th} Osprey's new position, $z_{j,k}^{P1}$ is the k^{th} dimension of the Osprey, G_j^{P1} is the objective value, $CF_{j,k}$ is the chosen fish for the j^{th} Osprey at the k^{th} dimension, and $I_{j,k}$ is the random number.

Exploitation: In this stage, the motion of the ospreys toward a safer position introduces slight adjustments in its location within the search space. These small variations enhance the exploitation ability and allow for a better local search and convergence toward optimal solutions.

In this optimizer, the Osprey's natural characteristic is simulated by first generating a new random position and safe location to consume its prey is given as:

$$z_{j,k}^{P2} = z_{j,k} + \frac{low_k + rand_{j,k} (up_k - low_k)}{s}$$
 (8)

where $s = \{1, 2, 3, ..., S\}$; s is the iteration count and S is the overall iterations.

$$z_{j,k}^{P2} = \begin{cases} z_{j,k}^{P2}, low_k \le z_{j,k}^{P2} \le up_k \\ low_k, z_{j,k}^{P2} \le low_k \\ up_k, z_{j,k}^{P2} > up_k \end{cases}$$
 (9)

where Z_j^{P2} is the j^{th} Osprey's new position, $z_{j,k}^{P2}$ is the k^{th} dimension of the Osprey,

When the updated position provides a better value, it replaces the osprey's prior position and it is expressed as:

$$Z_{j} = \begin{cases} Z_{j}^{P2}, G_{j}^{P2} < G_{j} \\ Z_{j}, elsewhere \end{cases}$$
 (10)

where G_j^{P2} is the objective value. Algorithm 1 shows the Pseudocode of the OOA to update the parameters of the DeepLabV3+.

Algorithm 1: Pseudocode of the OOA

Input: Population size, Ospreys and iterations

Output: Best Osprey Y_b

Initialize the population by Equations (5) and (6)

Evaluate the fitness by Equation (2)

For s = 1 to S

For k=1 to M

Stage 1: Exploration

Position of the fish is updated by $FP_i = \{Y_l \mid l \in \{1,2,3,...,M\} \land G_l < G_i\} \cup \{Y_b\}$

The new position within the search space is computed by $z_{i,k}^{P1} = z_{j,k} + rand_{j,k} \left(CF_{j,k} - I_{j,k} \times z_{j,k} \right)$

Initialize the boundary condition by $z_{j,k}^{P1} = \begin{cases} z_{j,k}^{P1}, low_k \le z_{j,k}^{P1} \le up_k \\ low_k, z_{j,k}^{P1} \le low_k \\ up_k, z_{j,k}^{P1} > up_k \end{cases}$

Update
$$j^{th}$$
 Osprey by $Z_j = \begin{cases} Z_j^{P1}, G_j^{P1} < G_j \\ Z_j, elsewhere \end{cases}$

Stage 2: Exploitation

Position of the fish is updated by $z_{j,k}^{P2} = z_{j,k} + \frac{low_k + rand_{j,k} (up_k - low_k)}{s}$

Initialize the boundary condition by $z_{j,k}^{P2} = \begin{cases} z_{j,k}^{P2}, low_k \leq z_{j,k}^{P2} \leq up_k \\ low_k, z_{j,k}^{P2} \leq low_k \\ up_k, z_{j,k}^{P2} > up_k \end{cases}$

Update
$$j^{th}$$
 Osprey by $Z_j = \begin{cases} Z_j^{P2}, G_j^{P2} < G_j \\ Z_j, elsewhere \end{cases}$

end

Save the best solution

4. RESULTS ANALYSIS

The following section show the results analysis of the proposed and existing model for showing the efficiency of the suggested work.

4.1. Implementation Details

The DeepLabV3+ model, integrated with OOA for brain tumor segmentation, is implemented using Python software. This process is executed on a computer running a 64-bit operating system, featuring 8 GB of RAM and Intel i5 processor. All experiments are demonstrated by 5-fold cross-validation for ensuring robustness. The reported outcomes represent the average performance across folds.

4.2. Datasets

There are two datasets like brain TCIA [20] and Figshare [21].

The brain MRI dataset consists of brain MRI scans accompanied by manually segmented Fluid Attenuated Inversion Recovery (FLAIR) abnormal images. The images were gathered from The Cancer Imaging Archive (TCIA) and have data from 110 patients. Each patient has at least one FLAIR sequence available. along with corresponding genomic clustered data.

The Figshare brain tumor data has 3,064 images obtained from 233 patients. It comprises 3 kinds of brain tumors: 708 images (meningioma), 1,426 images (glioma), and 930 images (pituitary tumor). Figure 3 shows the sample images of the TCIA and Figshare datasets.

4.3. Hyperparameters

Table 1 depicts the hyper-parameters of the suggested model. The backbone network is AlexNet, a learning rate of 0.001 and a weight decay of 0.0001 are chosen for proving stable convergence during training. For overcoming overfitting, a dropout rate of 0.3 is chosen, the Dice loss function is used, and the model is trained over 100 epochs to achieve optimal performance. The performance of the DeepLabV3+ model is based on fine-tuning of the several hyperparameters. Initially, default or manually chosen

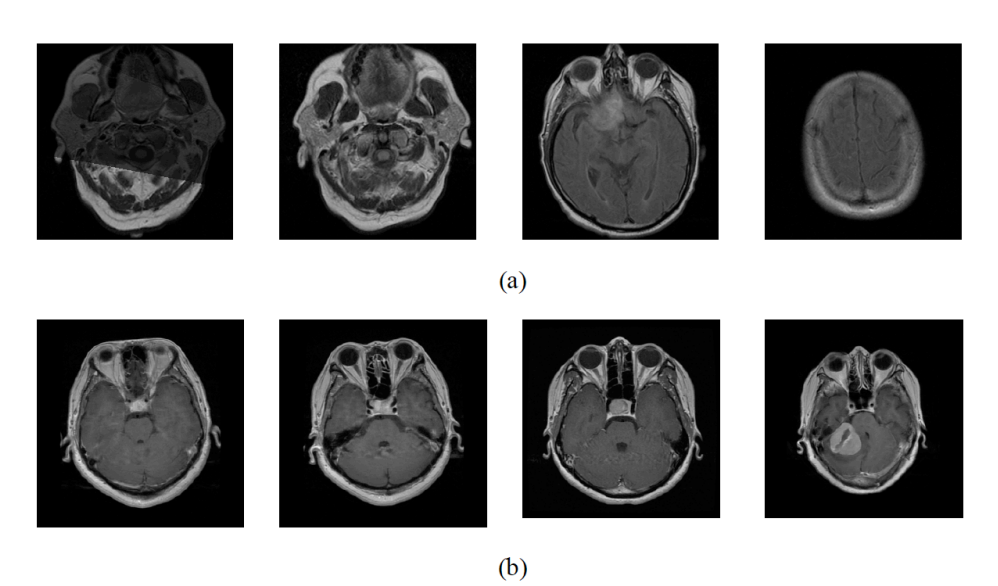


Figure 3: Sample images of the TCIA and Figshare datasets.

Table 1: Hyper-Parameters

Hyper-parameters	Before Optimization (Initial Value)	After OOA Optimization (Optimized Value)
Backbone Network	ResNet	AlexNet
Learning Rate	0.01	0.001
Weight Decay	0.0005	0.0001
Dropout Rate	0.5	0.3
Loss Function	Dice	Dice
Epochs	50	50

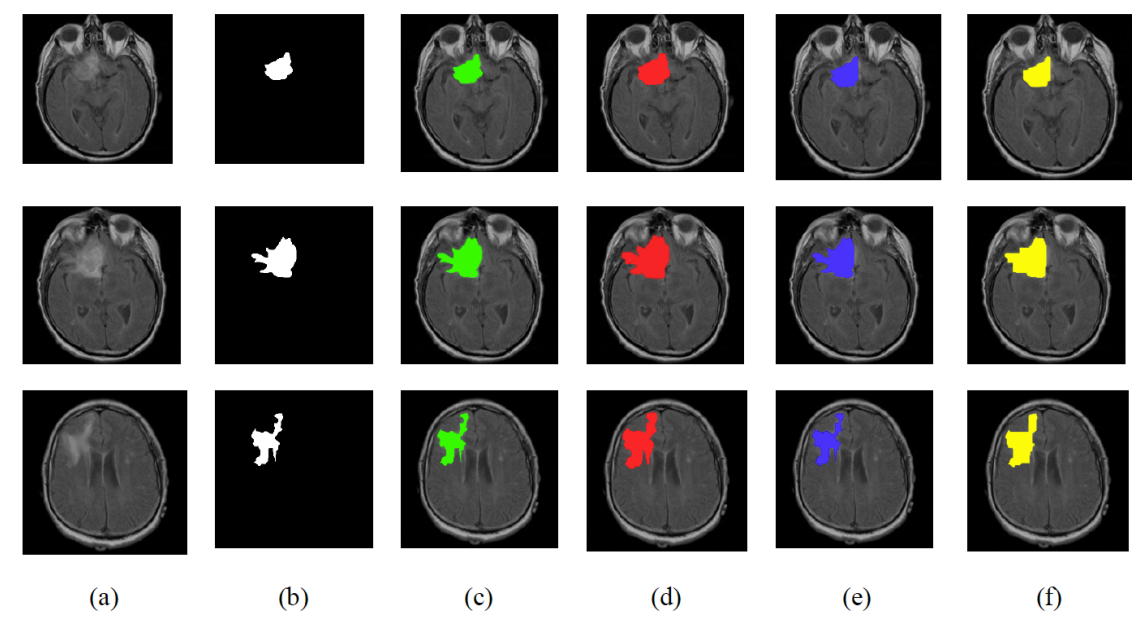


Figure 4: Analysis of (a) Input, (b) GT, (c) FCM, (d) UNet, (e) DeepLabV3 and (f) proposed on the TCIA dataset.

values are utilized for training. Finally, the network's optimization weights are performed using the OOA.

4.4. Qualitative Analysis

The following section shows the qualitative analysis on the two datasets like TCIA and Figshare. Here, the analysis is performance is evaluated for the approaches like FCM, UNet, DeepLabV3 and proposed (DeepLabV3+ with OOA).

Figures 4 and 5 delineates the qualitative analysis of input, Ground Truth (GT), FCM, UNet, DeepLabV3

and proposed (DeepLabV3+ with OOA) on the TCIA and Figshare datasets. The input images, Ground Truth (GT), and segmented outputs from all approaches are visually analyzed for assessing their accuracy in segmenting lesions. FCM, being a clustering based model, generally shows oversegmentation, the UNet and DeepLabV3 show improved segmentation but fails in boundary precision. Finally, the proposed DeepLabV3+ with OOA provided superior performance, preserved fine details and match with the GT. This shows its effectiveness in segmentation accuracy enhancement.

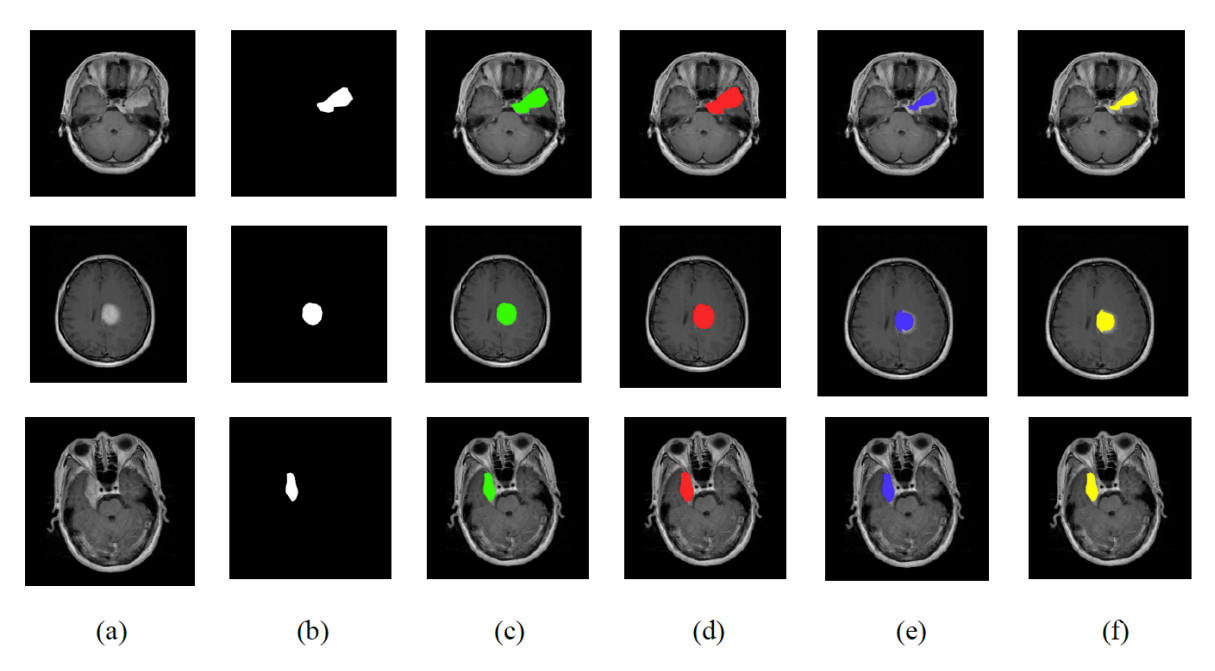


Figure 5: Analysis of (a) Input, (b) GT, (c) FCM, (d) UNet, (e) DeepLabV3 and (f) proposed on the Figshare dataset.

4.5. Ablation Study

The following section defines the ablation study with respect to the segmentation approaches like FCM, UNet, DeepLabV3 and proposed (DeepLabV3+ with OOA). Different performance measures like Accuracy, Sensitivity, Specificity, Precision, Dice and Intersection of Union (IoU) are compared.

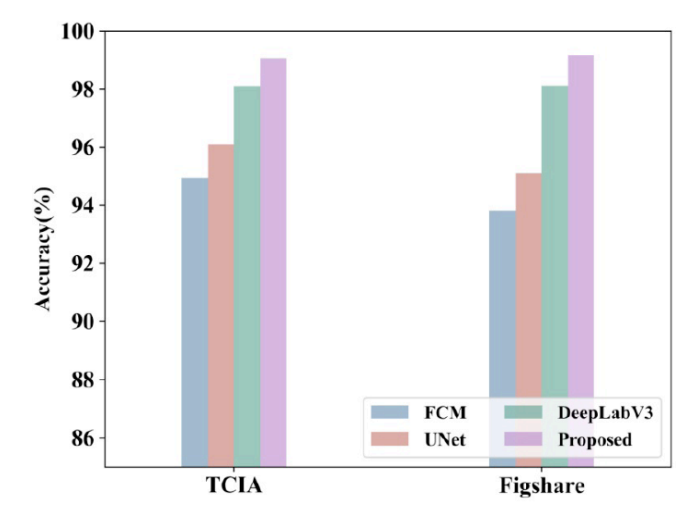


Figure 6: Accuracy comparison.

Figure 6 presents the accuracy comparison of different segmentation models like FCM, UNet, DeepLabV3 and proposed (DeepLabV3+ with OOA). Accuracy values attained by the FCM, UNet, DeepLabV3 and proposed models are 94.94%, 96%, 98.08% and 99.05% on the TCIA dataset. Similarly, an accuracy value achieved by the FCM is 93.8%, UNet is 95.1%. DeepLabV3 is 98.1% and proposed model is 99.14% on the Figshare dataset. By integrating the better feature extraction and segmentation capacity of DeepLabV3+ with the hyperparameter optimization strength of OOA, the suggested model attained superior performance in brain segmentation. The integration of OOA provides optimum weight tuning, improved boundary precision, high robustness to noise, and better convergence.

Figure 7 presents the precision comparison of different segmentation models like FCM, UNet, DeepLabV3 and proposed (DeepLabV3+ with OOA). A large precision value shows that the segmentation model is highly efficient at accurately showing the targeted regions without misclassifying irrelevant structures. Precision values attained by the suggested model are 99.12% (TCIA) and 99.09% (Figshare) datasets respectively.

Figure 8 presents the sensitivity comparison of different segmentation models like FCM, UNet,

DeepLabV3 and proposed (DeepLabV3+ with OOA). Sensitivity values attained by the FCM, UNet, DeepLabV3 and proposed models are 93.65%, 97.9%. 98.3% and 99.34% on the TCIA dataset. Then, sensitivity value achieved by the FCM is 95.87%, UNet is 97.7%, DeepLabV3 is 98.65% and proposed model is 99.42% on the Figshare dataset. These results presents that the merging of the OOA with DeepLabV3+ is major in refining the segmentation. The OOA assists in optimizing parameters of the model, and enhancing the feature extraction capabilities. Consequently, the proposed model outperformed conventional methods like FCM, UNet, DeepLabV3. This demonstrates its reliability and robustness in brain image segmentation process.

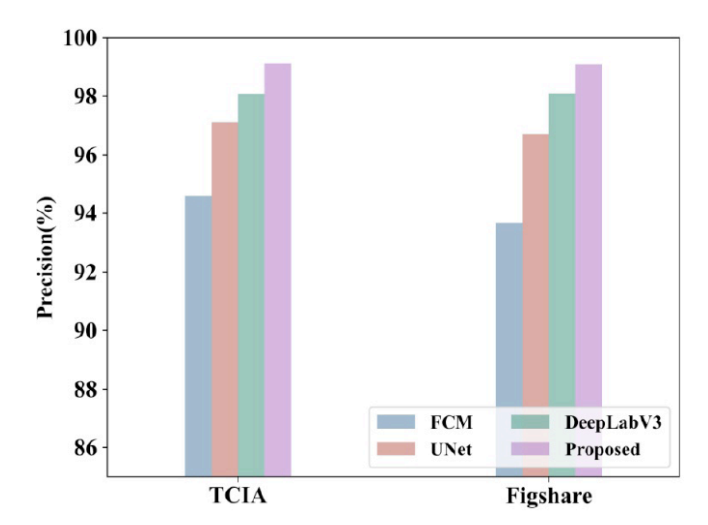


Figure 7: Precision comparison.

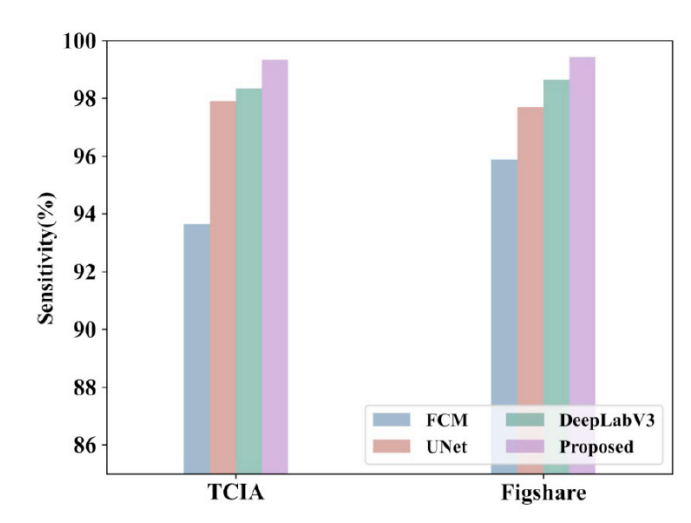


Figure 8: Sensitivity comparison.

Figure 9 presents the specificity comparison of different segmentation models. Higher value of specificity depicts that the model is efficiently differentiating relevant and non-relevant areas. The

suggested model maintained a better balance between detecting actual segmented areas. Specificity values attained by the suggested model are 99.59% (TCIA) and 99.3% (Figshare) datasets respectively.

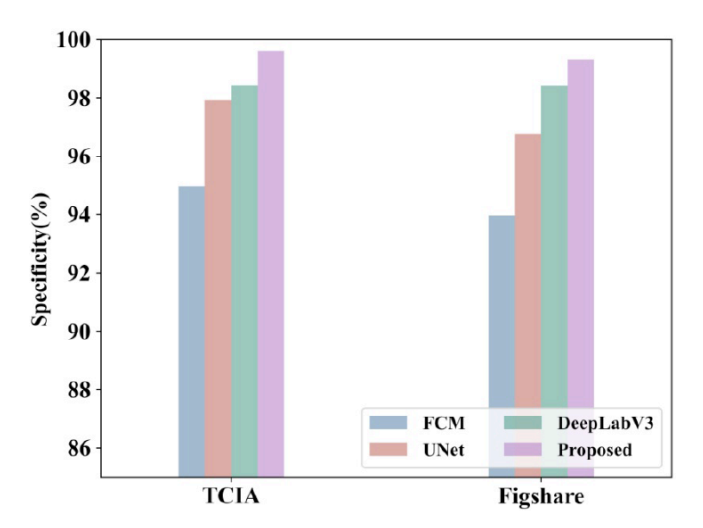


Figure 9: Specificity comparison.

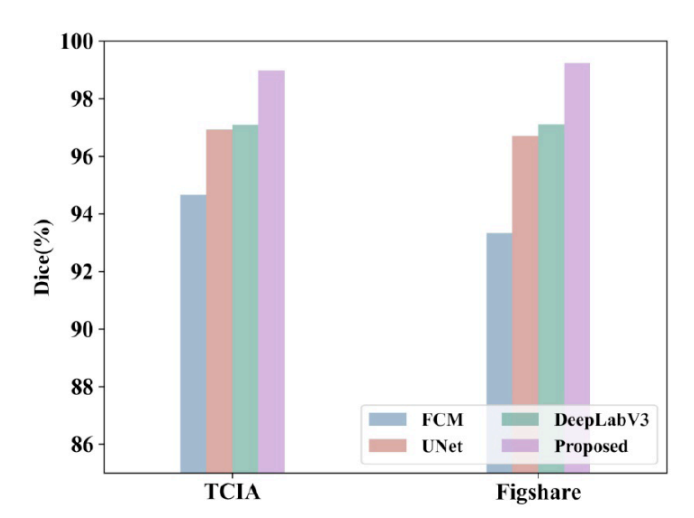


Figure 10: Dice comparison.

Figure **10** presents the dice comparison of different segmentation models. The high value of the dice score shows a greater degree of similarity among the segmented and the GT image. This analysis showcases how all approaches perform in terms of dice similarity. Dice values attained by the FCM, UNet, DeepLabV3 and proposed models are 94.65%, 96.91%, 97.08% and 98.97% on the TCIA dataset. Then, dice value achieved by the FCM is 93.3%, UNet is 96.7%, DeepLabV3 is 97.1% and proposed model is 99.23% on the Figshare dataset.

Figure 11 presents the IoU comparison of different segmentation models. The analysis shows every segmentation model performs with respect to the IoU and presenting their superiority in accurately finding and segmenting lesions. Conventional models like FCM, UNet, DeepLabV3 exhibited lower IoU scores because of their susceptibility to noise and difficulty in preserving fine details. IoU scores attained by the suggested model are 99.59% (TCIA) and 99.3% (Figshare) datasets respectively.

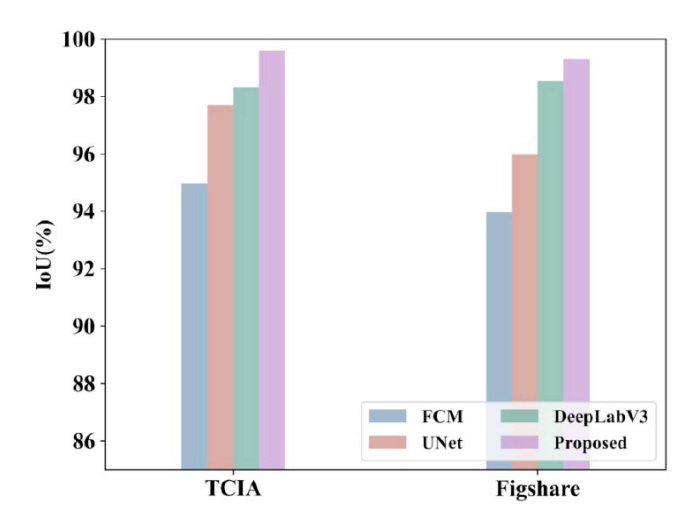


Figure 11: IoU comparison.

Table 2 presents the comparative of filtering methods, segmentation models, backbone networks, and optimization algorithms. NLM + Enhanced DeepLabV3+ (AlexNet + OOA) achieves the highest performance across all metrics. showing effectiveness of using NLM filtering with the Enhanced DeepLabV3+ model and OOA optimization. It is observed that NLM + Enhanced DeepLabV3+ (AlexNet + OOA) obtained the better performance across entire measures. This proves its effectiveness in brain tumor segmentation. Comparison with Gaussian and Median filtering, NLM better preserves structural details while reducing noise which lead to improved segmentation DeepLabV3+ accuracy. Further, with AlexNet outperformed other segmentation models like U-Net (ResNet-50) and DeepLabV3 with MobileNet or InceptionNet. When comparing optimization techniques, OOA provided superior outcomes over Genetic algorithm (GA), particle swarm Optimization (PSO), Arithmetic optimization algorithm (AOA) and Salp Swarm Optimization (SSA). This highlights its process in refining hyperparameters for optimal segmentation. These analyses proved that combining NLM filtering, Enhanced DeepLabV3+, AlexNet, and OOA optimization offers a better approach for efficient brain tumor segmentation and classification.

Table 3 illustrates the comparative analysis of different segmentation models with respect to different

Table 2: Comparative Analysis

Methods	Dice (%)	Accuracy (%)	Sensitivity (%)	Specificity (%)	Precision (%)	loU (%)
Gaussian Filter + DeepLabV3+ (AlexNet + GA)	97.32	98.76	97.83	98.94	97.58	92.71
NLM + DeepLabV3+ (VGG16 + PSO)	97.1	98.6	97.5	98.7	98.2	94.5
Median Filter + DeepLabV3 (MobileNet + OOA)	98.6	97.5	98.7	97.1	98.9	95.5
NLM + U-Net (ResNet-50 + AOA)	98.7	98.1	97.3	98.5	98.8	96.1
Median Filter + DeepLabV3 (InceptionNet + SSA)	98.9	98.4	97.9	98.7	99.0	97.4
Gaussian Filter + DeepLabV3+ (AlexNet + OOA)	98.7	98.1	98.3	99.1	98.8	97.9
NLM + Enhanced DeepLabV3+ (AlexNet + OOA)	99.23	99.14	99.42	99.3	99.09	99.3

Table 3: Performance Comparison with Statistical Validation

Methods	Dice (%) ± CI	Accuracy (%) ± CI	Sensitivity (%) ± CI	Specificity (%) ± CI	Precision (%) ±	IoU (%) ± CI
FCM	94.65 ± 0.42	94.94 ± 0.38	93.65 ± 0.51	95.12 ± 0.47	94.72 ± 0.44	90.21 ± 0.39
UNet	96.91 ± 0.35	96.00 ± 0.33	97.90 ± 0.40	97.25 ± 0.41	97.01 ± 0.38	92.10 ± 0.37
DeepLabV3	97.08 ± 0.28	98.08 ± 0.29	98.30 ± 0.31	98.40 ± 0.32	98.15 ± 0.28	95.30 ± 0.30
Proposed (DeepLabV3+ + OOA, TCIA)	98.97 ± 0.25	99.05 ± 0.22	99.34 ± 0.27	99.59 ± 0.21	99.12 ± 0.23	99.59 ± 0.24
Proposed (DeepLabV3+ + OOA, Figshare)	99.23 ± 0.21	99.14 ± 0.20	99.42 ± 0.24	99.30 ± 0.22	99.09 ± 0.21	99.30 ± 0.22

measures. Each value is reported as mean ± 95% confidence interval, averaged over 5-fold crossvalidation. The outcomes proved that the proposed method achieved the highest performance across all evaluation measures, with Dice scores of 98.97% (TCIA) and 99.23% (Figshare). Table 4 compares the training time per epoch and memory usage of different models. The proposed DeepLabV3+ with OOA achieved the best trade-off and required only 21.2 seconds per epoch and 2.1 GB of memory. Thus, the proposed method is more accurate and computationally efficient.

4.6. Comparison with Recent Works

Table 5 shows the comparative analysis with different works like [12-18] with the proposed model. It is noted from the analysis that the suggested model outperformed all the approaches due to the integration of DeepLabV3+ and OOA. Thus, it is proved that the suggested approach can be utilized for brain tumor diagnosis. The comparison of brain techniques highlights three main segmentation approaches: handcrafted features, CNN-based methods, and hybrid approaches. Handcrafted feature methods benefit from domain knowledge and are

Table 4: Comparison of Computational Cost

Models	Training Time / Epoch (s)	Memory Usage (GB)	
FCM	25.1	3.5	
UNet	110.6	4.2	
DeepLabV3	150.3	4.8	
Proposed (DeepLabV3+ + OOA)	21.2	2.1	

Table 5: Comparison with Recent Works

References	Dice (%)	Accuracy (%)	Sensitivity (%)	Specificity (%)	Precision (%)	IoU (%)
[12]	95	-	-	-	-	-
[13]	91.87	-	92.29	99	-	84.96
[14]	91	-	93	-	96	84
[15]	81.42	99.12	80	98	-	-
[16]	-	98.9	-	-	-	-
[17]	-	96	-	-	96	-
[18]	-	98.6	-	-	-	-
Proposed (TCIA)	98.97	99.05	99.34	99.59	99.12	99.59
Proposed (Figshare dataset)	99.23	99.14	99.42	99.3	99.09	99.3

compatible with traditional machine learning algorithms. However, they are sensitive to intensity variations and require manual tuning, which can limit scalability and performance. CNN-based methods offer automatic feature learning, robustness to intensity changes, and deliver high precision and accuracy. Despite these strengths, they are computationally expensive, depend on large annotated datasets, and may lack interpretability. Hybrid approaches aim to combine the advantages of both handcrafted and CNN-based techniques, leading to improved performance and potentially greater interpretability.

5. DISCUSSION

The proposed DeepLabV3+ integrated with the OOA shown better segmentation performance compared to methods FCM, UNet, and baseline DeepLabV3. Instead of focusing only on the quantitative improvements, the significance of these outcomes is based on their potential clinical impact. By achieving more precise boundary representation and more robust to noise, the method could provide radiologists with more reliable tumor localization. Further, it supports decision-making, diagnostic errors, and improves treatment planning. Moreover, the near-real-time execution of the model suggests the feasibility of deployment in hospital workflows, where automated assistance could improve MRI analysis and overcomes workload of the radiologists.

Although, promising results has been achieved by the suggested model, certain limitations must be acknowledged. First, the present work is on the basis of the 2D MRI slices, which may not entirely capture volumetric tumor characteristics. The suggested model will be extended to 3D volumetric segmentation would provide more comprehensive spatial information for diagnosis. Second, even though the model performed well on TCIA and Figshare datasets, the dataset sizes remain relatively modest for requirements of the DL model. This raise problem about the generalizability of the model to larger and more diverse clinical populations. Third, the absence of external clinical validation restricts the direct applicability of the model in real-time hospital settings. Addressing these limitations through multimodal MRI integration, larger-scale datasets, and external validation studies will be major stages to clinical translation.

6. CONCLUSION

This work presented an enhanced model to segment and classifies the brain tumors using the DeepLabV3+ with OOA model. in the DeepLabV3+ model, the AlexNet was considered as the backbone. The integration of this approach has significantly enhanced the brain tumor segmentation performance by optimizing model parameters and enhancing feature extraction. The AOO further optimized hyperparameters of the DeepLabV3+ and ensured better segmentation performance. Comparison of the suggested model with existing models like FCM, UNet, and DeepLabV3, provided that the proposed method obtained superior performance with respect to different measures on two datasets. As a result, the suggested model achieved better segmentation and suitable for real-time analysis. The present segmentation is performed on 2D MRI slices. Future work will focus on extending the suggested model to multimodal MRI for

capturing complementary information across imaging modalities, investigating more diverse clinical datasets. robustness. generalizability. This provides investigating real-time deployment in clinical workflows for supporting radiologists in practice. Moreover, method toward expanding the 3D segmentation and explainable AI techniques will further improve clinical relevance and interpretability.

CONSENT FOR PUBLICATION

Not applicable.

FUNDING

None.

CONFLICT OF INTEREST

The authors declare no conflict of interest, financial or otherwise.

AVAILABILITY OF DATA

The findings of this systematic review are based on publicly available articles from PubMed, Web of Science, and Scopus. The detailed raw data can be found in the original studies listed in our references. Anyone who needs further information or specific data should check the original publications or contact the authors. This respective approach ensures transparency and allows others to validate and replicate our results.

REFERENCE

- [1] Pani K, Chawla I. A hybrid approach for multi modal brain tumor segmentation using two phase transfer learning, SSL and a hybrid 3DUNET. Computers and Electrical Engineering 2024; 118: 109418. https://doi.org/10.1016/j.compeleceng.2024.109418
- Jamazi C, Manita G, Chhabra A, Manita H, Korbaa O. [2] Mutated Aquila Optimizer for assisting brain tumor segmentation. Biomedical Signal Processing and Control 2024; 88: 105089. https://doi.org/10.1016/j.bspc.2023.105089
- An D, Liu P, Feng Y, Ding P, Zhou W, Yu B. Dynamic [3] weighted knowledge distillation for brain tumor segmentation. Pattern Recognition 2024; 155: 110731. https://doi.org/10.1016/j.patcog.2024.110731
- Jyothi P, Robert Singh A. Deep learning models and [4] traditional automated techniques for brain segmentation in MRI: a review. Artificial Intelligence Review 2023; 56(4): 2923-2969. https://doi.org/10.1007/s10462-022-10245-x
- Ranjbarzadeh R, Caputo A, Tirkolaee EB, Ghoushchi SJ, [5] Bendechache M. Brain tumor segmentation of MRI images: A comprehensive review on the application of artificial intelligence tools. Computers in Biology and Medicine 2023; 152: 106405. https://doi.org/10.1016/j.compbiomed.2022.106405

- Zhu Z, He X, Qi G, Li Y, Cong B, Liu Y. Brain tumor segmentation based on the fusion of deep semantics and edge information in multimodal MRI. Information Fusion 2023; 91: 376-387. https://doi.org/10.1016/j.inffus.2022.10.022
- Saifullah S, Dreżewski R, Yudhana A, Wielgosz M, [7] Caesarendra W. Modified U-Net with attention gate for enhanced automated brain tumor segmentation. Neural

Computing and Applications 2025; 37(7): 5521-5558.

https://link.springer.com/article/10.1007/s00521-024-10919-3

- Qin J, Xu D, Zhang H, Xiong Z, Yuan Y, He K. BTSegDiff: [8] Brain tumor segmentation based on multimodal MRI Dynamically guided diffusion probability model. Computers in Biology and Medicine 2025; 186: 109694.
 - https://doi.org/10.1016/j.compbiomed.2025.109694
- Md Islam M, Md Alamin T, Md Ashraf U, Arnisha A, Majdi K. [9] Brainnet: Precision brain tumor classification with optimized efficientnet architecture. International Journal of Intelligent Systems 2024; 2024(1): 3583612. https://doi.org/10.1155/2024/3583612
- [10] Jena B, Nayak GK, Saxena S. An empirical study of different machine learning techniques for brain tumor classification and subsequent segmentation using hybrid texture feature. Machine Vision and Applications 2022; 33(1): 6. https://doi.org/10.1007/s00138-021-01262-x
- [11] Balaha HM, Hassan AS. A variate brain tumor segmentation, optimization, and recognition framework. Artificial Intelligence Review 2023; 56(7): 7403-7456. https://doi.org/10.1007/s10462-022-10337-8
- [12] Cheng Y, Zheng Y, Wang J. CFNet: Automatic multi-modal brain tumor segmentation through hierarchical coarse-to-fine fusion and feature communication. Biomedical Signal Processing and Control 2025; 99: 106876. https://doi.org/10.1016/j.bspc.2024.106876
- Mi J, Zhang X. Diffusion network with spatial channel [13] attention infusion and frequency spatial attention for brain tumor segmentation. Medical Physics 2025; 52(1): 219-231. https://doi.org/10.1002/mp.17482
- Cekic E, Pinar E, Pinar M, Dagcinar A. Deep learning-[14] assisted segmentation and classification of brain tumor types on magnetic resonance and surgical microscope images. World Neurosurgery 2024; 182: e196-e204. https://doi.org/10.1016/j.wneu.2023.11.073
- Farnoosh R, Noushkaran H. Development of an [15] unsupervised pseudo-deep approach for brain tumor detection in magnetic resonance images. Knowledge-Based Systems 2024; 300: 112171. https://doi.org/10.1016/j.knosys.2024.112171
- Ramtekkar PK, Pandey A, Pawar MK. Innovative brain tumor [16] detection using optimized deep learning techniques. International Journal of System Assurance Engineering and Management 2023; 14(1): 459-473. https://doi.org/10.1007/s13198-022-01819-7
- [17] Devi RS, Perumal B, Rajasekaran MP. A hybrid deep learning based brain tumor classification and segmentation by stationary wavelet packet transform and adaptive kernel fuzzy c means clustering. Advances in Engineering Software 2022: 170: 103146. https://doi.org/10.1016/j.advengsoft.2022.103146
- Mehnatkesh H, Jalali SMJ, Khosravi A, Nahavandi S. An [18] intelligent driven deep residual learning framework for brain tumor classification using MRI images. Expert Systems with Applications 2023; 213: 119087. https://doi.org/10.1016/j.eswa.2022.119087
- Dehghani M, Trojovský P. Osprey optimization algorithm: A new bio-inspired metaheuristic algorithm for solving engineering optimization problems. Frontiers in Mechanical Engineering 2023; 8: 1126450. https://doi.org/10.3389/fmech.2022.1126450

- [20] Buda M, Saha A, Mazurowski MA. Association of genomic subtypes of lower-grade gliomas with shape features automatically extracted by a deep learning algorithm. Computers in Biology and Medicine 2019; 109: 218-225. https://doi.org/10.1016/j.compbiomed.2019.05.002
- [21] Deepak S, Ameer PM. Brain tumor classification using deep CNN features via transfer learning. Computers in Biology and Medicine 2019; 111: 103345. https://doi.org/10.1016/j.compbiomed.2019.103345

Received on 15-07-2025 Accepted on 11-08-2025 Published on 07-09-2025

https://doi.org/10.30683/1929-2279.2025.14.15

© 2025 Jacob and Winston; Licensee Neoplasia Research.

This is an open-access article licensed under the terms of the Creative Commons Attribution License (http://creativecommons.org/licenses/by/4.0/), which permits unrestricted use, distribution, and reproduction in any medium, provided the work is properly cited.